J Cancer Res Clin Oncol (2000) 126:325–331

ORIGINAL PAPER

Martin C. Jäckel · Petra Köpf-Maier · Frank Baumgart
Dieter Ziessow · Robert Tausch-Treml

Value of ^{31}P NMR spectroscopy in predicting the response of a xenografted human hypopharynx carcinoma to irradiation

Received: 26 July 1999 / Accepted: 29 December 1999

Abstract ***Purpose:*** An early indicator of tumor sensitivity to irradiation could provide useful information on the effectiveness of therapy and may facilitate more individual designs of treatment protocols. The aim of the present study was to evaluate the potential of in vivo ^{31}P nuclear magnetic resonance spectroscopy in predicting the response of a xenografted human hypopharynx carcinoma to radiotherapy. ***Methods:*** The tumor had been serially heterotransplanted to athymic mice. ^{31}P NMR spectra were collected before and at four intervals (24, 48, 72, and 120 h) after irradiation with 15 Gy or 30 Gy. Alterations of phosphorus metabolism were compared with the growth delays, the histological appearance, and the mitotic activity of the treated tumors. ***Results:*** Radiation with 30 Gy induced increases of the phosphodiester level ($P < 0.001$) as well as of the tumor pH ($P < 0.05$) and decreases of the phosphomonoester level ($P < 0.001$) within 48 h. The changes clearly preceded measurable tumor responses and were accompanied by severe histological destruction and marked depression of mitotic indices. However, none of these spectral alterations was significantly correlated with individual delays of tumor growth. The only parameters allowing a prediction of radiation-induced tumor responses were the pre-treatment levels of phosphomonoesters and -diesters. The ^{31}P NMR spectroscopic changes observed after therapy with 15 Gy were either unsystematic or insignificant. ***Conclusions:*** Pretreatment levels of tumor phospholipids were indicative of radiosensitivity in the xenografted human hypopharynx carcinoma investigated here. However, since phosphorus metabolism varies considerably among different tumor lines, it seems unlikely that there exists a uniform ^{31}P NMR spectroscopic parameter predicting tumor response to radiation therapy.

Key words ^{31}P NMR spectroscopy · Hypopharynx carcinoma · Radiotherapy

Abbreviations *PCr* phosphocreatine · *PME* phosphomonoesters · *PDE* phosphodiesters · P_i inorganic phosphate · *TPC* total phosphorus content

This work was supported by a grant from the Dr. Milded Scheel Stiftung, Deutsche Krebshilfe e.V., Bonn, Germany

M. C. Jäckel (✉)
Department of Otorhinolaryngology, University of Göttingen,
Robert-Koch-Str. 40, D-37075 Göttingen, Germany
Tel.: +49-551-392802
Fax: +49-551-392809

P. Köpf-Maier
Institut für Anatomie, Free University of Berlin,
Königin-Luise-Str. 15, D-14195 Berlin, Germany

F. Baumgart · D. Ziessow
Iwan-N.-Stranski-Institut, Technical University of Berlin,
Straße des 17. Juni 135, D-10623 Berlin, Germany

R. Tausch-Treml
Department of Otorhinolaryngology,
Martin-Luther-University of Halle-Wittenberg,
Magdeburger Str. 12, D-06097 Halle, Germany

Introduction

Phosphorus nuclear magnetic resonance (^{31}P NMR) spectroscopy measures the relative levels of cellular phosphate compounds that play an important role in tissue metabolism. It provides information on bioenergetic metabolites such as nucleoside triphosphates (NTP), phosphocreatine (PCr), and inorganic phosphate (P_i), as well as on phosphomonoesters (PME) and phosphodiesters (PDE), which are known to be involved in lipid synthesis for biological membranes (Van den Bosch 1974). Localized ^{31}P NMR spectroscopy can be performed in animals and humans in a non-invasive manner. Its greatest potential in oncology is that it can permit a non-invasive monitoring of tumor response to radio-, chemo-, or immunotherapy. A number of previous reports have focused on the changes observed in ^{31}P NMR spectra of murine and human tumors following irradiation. Their results, however, have been inconclusive, indicating variable changes of high-energy

phosphates (Kristjansen et al. 1990; Mahmood et al. 1995; Merchant et al. 1995; Murata et al. 1998; Sakurai et al. 1998; Sijens et al. 1986, 1997) and/or phospholipid metabolites (Mahmood et al. 1995; Sakurai et al. 1998; Sijens et al. 1986; Street and Koutcher 1997). Only a few studies have found tumor responses to be related to radiation-induced metabolic changes (Kristjansen et al. 1990; Murata et al. 1998; Sijens et al. 1997) or with the pre-treatment status of phosphorus metabolism (Fu et al. 1990; Li et al. 1995).

At the time of diagnosis, about 30% of patients with squamous cell carcinoma of the upper aerodigestive tract suffer from advanced disease that is hardly or not at all resectable (Snow 1992). In this situation, primary irradiation with or without concurrent chemotherapy may be a promising treatment modality today. Owing to their superficial location, head and neck carcinomas are particularly suited for monitoring the phosphorus metabolism of tumors before, during, and after therapy by ^{31}P NMR spectroscopy. Clinical studies performed so far, however, have yielded conflicting results, possibly because of the small number and the heterogeneity of patients investigated and of difficulties in the timing of the spectroscopic measurements (Karczmar et al. 1991; Maldonado et al. 1998; Tausch-Treml et al. 1992b; Vogl et al. 1989).

In the present study, a heterotransplanted human hypopharynx carcinoma was used to investigate the value of in vivo ^{31}P NMR spectroscopy in predicting tumor response to radiotherapy. Compared with murine tumors, on which the majority of previous studies have been performed, this model more closely corresponds to clinical conditions and might provide clues to the usefulness of this method in patients with head and neck carcinoma. On the other hand, the experimental setting largely enables one to circumvent the drawbacks of clinical investigations, as mentioned above. Alterations in phosphorus metabolism were studied as a function of dose and time following irradiation and were related to the growth delay and the histological appearance of the tumors.

Materials and methods

Tumor model

The investigations were performed on a moderately differentiated squamous cell carcinoma of the hypopharynx originating from a previously untreated patient. It was serially heterotransplanted in male athymic mice (NMRI, nu/nu) as described previously (Tausch-Treml et al. 1991). Animals were kept in autoclaved cages set in laminar-airflow racks; food and acidified water (pH 2.5) were provided ad libitum. At the time of transplantation the animals were 6–8 weeks old and weighed approximately 25 g. Tumor volumes were estimated by caliper measurements of two perpendicular parameters (length a, breadth b) and calculations according to the formula for the volume of ellipsoids ($0.5 \times a \times b^2$). Around day 25 after transplantation, when the experiments were initiated, the tumors had reached an average volume of 1.54 ± 0.35 cm^3 and showed maximal growth with a doubling time of about 6 days. This tumor size was necessary to obtain ^{31}P NMR spectra of a sufficiently good quality. Following irradiation, the time t_{150}, after which a tumor had grown to 150% of its size before therapy, was determined by daily measurements of tumor volumes. Tumor growth delay was defined as the difference between averaged t_{150} values obtained for treated and untreated tumors.

Irradiation

Radiation was delivered by a Siemens-Stabilipan, which operated at 180 kV and 20 mA, and had a 0.5-mm Cu filter and a cone diameter of 2.0 cm. The dose rate at the end of the cone was 2.07 Gy/min. Before irradiation, the mice were anesthetized by a shallow neuroleptic analgesic composed of 0.05 mg/kg fentanyl base, 0.25 mg/kg droperidole, and 0.25 mg/kg diazepam. To prevent excessive X-ray damage to normal tissues, the surroundings of the tumors were shielded by 1-mm-thick lead. Radiation was administered at doses of 15 Gy or 30 Gy.

NMR spectroscopy

For in vivo NMR measurements, the mice were anesthetized in the same manner as for X-irradiation. ^{31}P NMR spectra were obtained with a Bruker Biospec (40-cm horizontal bore) at 2.35 T. Home-built probes with a three-turn surface coil (11 mm diameter), doubly tuned to ^{31}P and ^{1}H, were used for the experiments. Tumor spectra were obtained by placing the coil in contact with the tumor. To ascertain that normal tissues underlying the subcutaneously growing tumors did not contribute to the tumor-derived NMR spectra, mice without a tumor were measured in the same position in the probe as tumor-bearing mice. An ellipsoid-shaped silicone bag with a volume of 0.8 cm^3, filled with saline, served as a phantom tumor and was placed between the coil and the mouse in order to create similar coil-loading conditions to those experienced with a tumor. Tumor spectra were taken before treatment and at intervals of 24, 48, 72, 120 h after irradiation.

The ^{31}P NMR spectral parameters were defined by a resonance frequency of 40.63 MHz, a 50° flip angle, 4-kHz bandwidth, 10^3 data points, 2 s recycle time, and 750 scans. No corrections were made for saturation effects. Each free induction decay was processed by 15-Hz line broadening. For analyzing the spectra, individual resonance-area integrals were employed by using a Lorentzian line-fitting program. The tumor pH was calculated from the chemical shift of P_i. ^{31}P chemical shifts were reported in relation to the resonance of phosphocreatine at 0 ppm when it was present, or to α-NTP at −7.57 ppm when phosphocreatine was not identifiable.

For statistical analysis, the two-tailed paired t-test was applied when tumors within one treatment group were compared. A rank correlation was used for estimating the correlation coefficients.

Light microscopy

Parallel to the NMR experiments, histological investigations were performed. For this purpose, groups of 12 mice bearing size-matched tumors were irradiated with 15 Gy or 30 Gy. At the same intervals as were used for NMR measurements, two animals were killed in each case, their tumors were removed and were immersed for 2 days in Karnofsky's solution containing 3% paraformaldehyde and 3.75% glutaraldehyde in cacodylate buffer (pH 7.4). After postfixation in 1% osmium tetroxide for 1 h, they were dehydrated through graded alcohols and embedded in Epon. Sections cut at a thickness of 0.8–1 μm were stained with toluidine blue. For determination of mitotic indices, the number of mitoses in 2000 cells/sample were counted.

Results

NMR spectra during untreated tumor growth

Figure 1 gives an example of the ^{31}P NMR spectrum obtained from an untreated individual hypopharynx

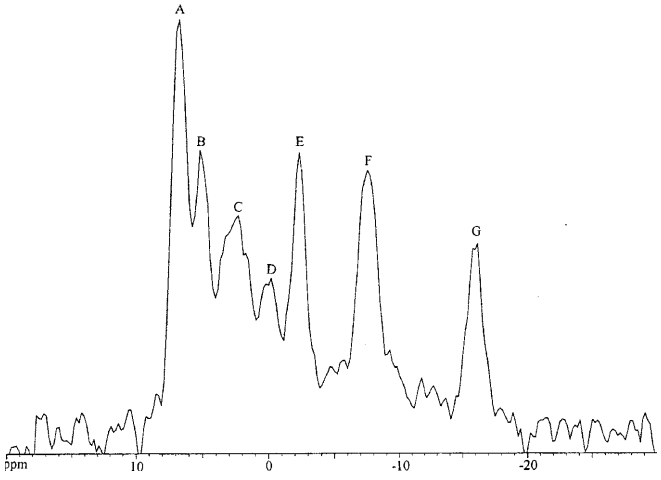

Fig. 1 Typical in vivo ^{31}P NMR spectrum of an untreated hypopharynx carcinoma xenograft on day 25 after tumor inoculation (tumor volume: 1.35 cm^3). Resonance assignments: *A* phosphomonoester (PME), *B* inorganic phosphate (P_i), *C* phosphodiester (PDE), *D* phosphocreatine (PCr), *E* γ-NTP, *F* α-NTP, *G* β-NTP

carcinoma xenograft. It comprises diverse peaks representing the relative levels of phosphate compounds in the tumor tissue. A significant contribution of signals deriving from the body wall has been excluded in preliminary experiments performed with a 0.8-cm^3 phantom tumor. To analyze the alterations occurring during uninfluenced growth, the metabolite ratios were related to the total phosphorus content (TPC) seen in the spectrum and were normalized to the values observed on day 25 after tumor inoculation (Fig. 2b; $n = 6$ animals). The most significant changes were increases of the PME/TPC and the PDE/TPC ratios ($P < 0.01$) detectable within 2 days. As described previously, the PME peak has been assigned to phosphocholine and phosphoethanolamine while the PDE peak consisted of glycerophosphocholine and glycerophosphoethanolamine (Tausch-Treml et al. 1992a). In parallel, a moderate decrease of the PCr/TPC quotient ($P < 0.05$) appeared. The pH value of the tumor tissue and the P_i/TPC ratio remained nearly unchanged (data not shown).

NMR spectra following irradiation

Irradiation with doses of 15 Gy ($n = 12$ animals) or 30 Gy ($n = 13$ animals) resulted in a temporary decline of tumor volumes, whereafter a regrowth of the transplants occurred (Fig. 2a). The tumor growth delays induced by the two irradiation doses differed significantly from each other (321 ± 68 h versus 476 ± 86 h, $P < 0.001$). Figure 2c demonstrates the alterations of metabolites visible by ^{31}P-NMR observed after irradiation with 30 Gy. The most remarkable change was a highly significant increase of the PDE/TPC ratio that occurred immediately after treatment and reached a maximum at 48 h ($P < 0.001$). During the same period,

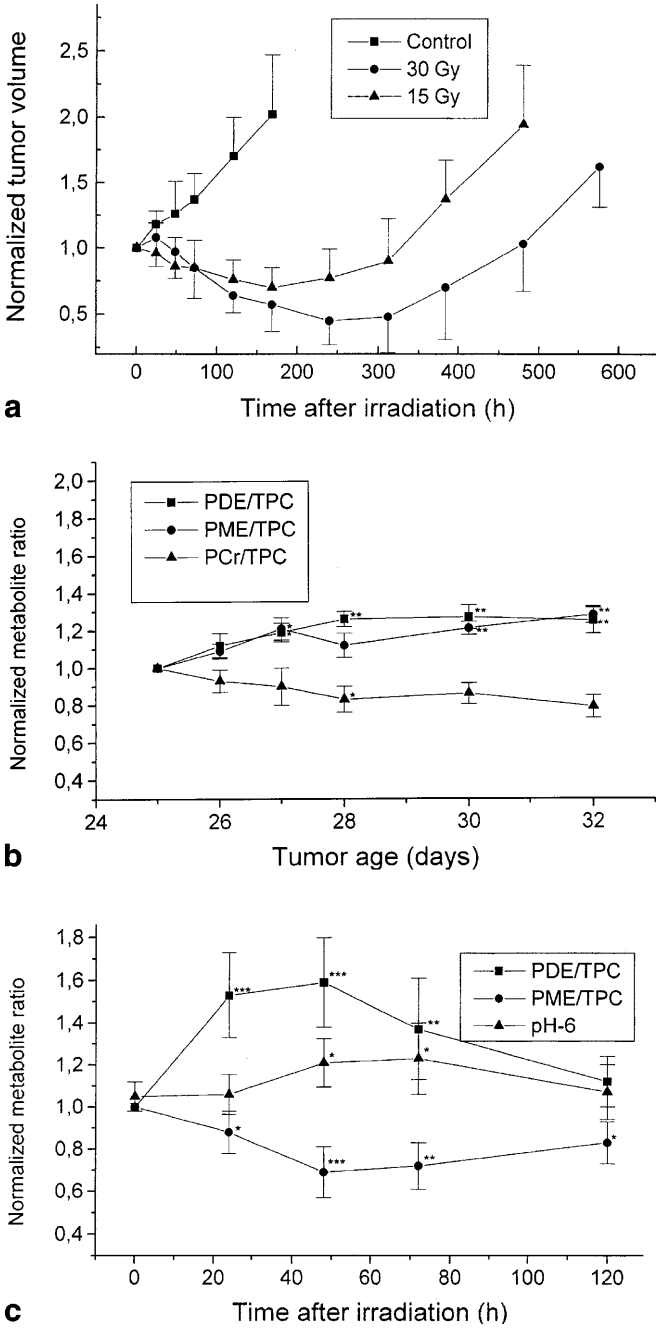

Fig. 2a–c Tumor growth of the untreated and treated hypopharynx carcinoma (**a** $n = 3 \times 6$ animals), changes of phosphorus metabolite ratios observed in untreated control tumors (**b** $n = 6$ animals), and changes observed in tumors irradiated with 30 Gy (**c** $n = 13$ animals). All values are normalized to those obtained on day 25 after tumor inoculation, on which radiotherapy was applied to the treatment group. The pH is given as the actual number with an initial value of pH = 6. Asterisks indicate significant changes of metabolite ratios or pH compared to the respective initial values (*$P < 0.05$; **$P < 0.01$; ***$P < 0.001$)

the PME/TPC ratio diminished ($P < 0.001$), while the pH value slightly rose ($P < 0.05$). Other metabolites showed either unsystematic changes (NTP/TPC) or insignificant increases (PCr/TPC) or decreases of their levels (P_i/TPC; data not shown). Radiation with 15 Gy

Table 1 Linear regression coefficients (r) between the tumor growth delays and the pre-treatment metabolite ratios (*upper part*) and the changes of the metabolite ratios following irradiation with 30 Gy (*lower part*). *PCr* phosphocreatine, *TPC* total phosphorus content, P_i inorganic phosphate, *PME* phosphomonoesters, *PDE* phosphodiesters

Parameter	r
Pretreatment metabolite ratio	
PCr/TPC	0.07
P_i/TPC	0.39
PME/TPC	−0.61*
PDE/TPC	−0.48
Pretreatment pH	0.21
Change of metabolite ratio	
PME/TPC	
24 h	−0.15
48 h	−0.09
PDE/TPC	
24 h	0.41
48 h	0.30
Change of pH (48 h)	0.12

*$P < 0.05$

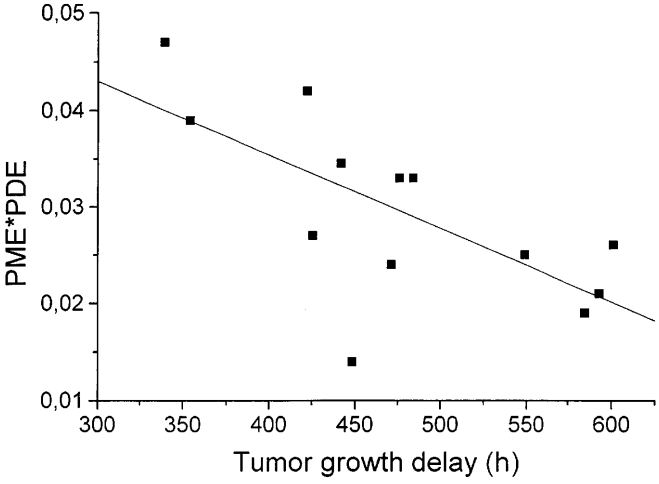

Fig. 3 Scatter diagram demonstrating the relationship between growth delays of individual tumors after irradiation with 30 Gy and the product of the respective pre-treatment PME/total phosphorus content (TPC) and PDE/TPC ratios (*PME*PDE*). Linear regression analysis revealed a significant negative connection with a coefficient $r = -0.69$ ($P < 0.01$)

produced similar metabolic perturbations that did not reach statistical significance (data not shown).

To evaluate whether the individual tumor regressions correlated with the individual ^{31}P NMR spectrometric data, the metabolite ratios seen before irradiation as well as the changes of the metabolite ratios occurring after irradiation were related to the observed tumor growth delays. Table 1 gives the respective correlation coefficients found for the group of mice irradiated with 30 Gy. The pretreatment PME/TPC and PDE/TPC ratios were correlated with poor tumor response to therapy; the latter, however, was just at a borderline significance level ($P < 0.05$ and $P < 0.1$ respectively). When the two parameters were multiplied by each other, the negative relationship with tumor growth delay improved to a regression coefficient of $r = -0.69$ ($P < 0.01$; Fig. 3). The changes of the metabolite ratios after treatment did not show any significant association with individual tumor responses. Only the extent of the increase of the PDE/TPC ratio was weakly related to the degree of tumor regression. For the group of mice treated with 15 Gy, neither pre- nor post-treatment metabolite ratios were significantly associated with the individual growth delays of tumors (data not shown).

Morphology following irradiation

Figure 4a illustrates the morphology of an untreated control tumor. It represents a moderately differentiated squamous cell carcinoma with tumor cell clusters imitating the structure of the spinocellular stratum of the epidermis. The tumor cells were organized as reticularly arranged cell cords that encircled wide central areas containing necrotic cells, the number of which gradually increased during uninfluenced tumor growth. When the experiments started, the averaged mitotic index in the untreated tumor tissue amounted to 4.1 ± 0.4%.

Following irradiation with 30 Gy, the number of mitotic figures markedly decreased within 2 days (Fig. 5). In parallel, many tumor cells developed signs of cellular damage including cytoplasmic lipid droplets, lysosomal bodies, and condensation of the nuclear chromatin (Fig. 4b). On days 3 and 4 after irradiation, an increasing number of necrotic cells appeared within the tumor cell cords, the histological organization of which largely destroyed (Fig. 4c). Finally, a regrowth of tumor cells took place on days 5 and 6 and was accompanied by an increment of mitotic activity (Figs. 4d, 5).

Analogous but less severe morphological alterations occurred in the tumor tissue when irradiation doses of 15 Gy were applied. As observed after high-dose therapy, the phenomena were most pronounced on day 3 after treatment (sections not shown). Simultaneously, a drop of mitotic activity became evident within 2 days (Fig. 5).

Discussion

Several investigators have previously examined the phosphorus metabolism in carcinomas after irradiation by ^{31}P NMR spectroscopy. They reported a variety of changes that apparently depended on the tumor types investigated and on the irradiation doses applied. Most studies confirmed a rise of high-energy phosphates, as shown by increasing PCr/P_i and/or β-NTP/P_i ratios after irradiation (Mahmood et al. 1995; Majors et al. 1990; Merchant et al. 1995; Sakurai et al. 1998). Other inves-

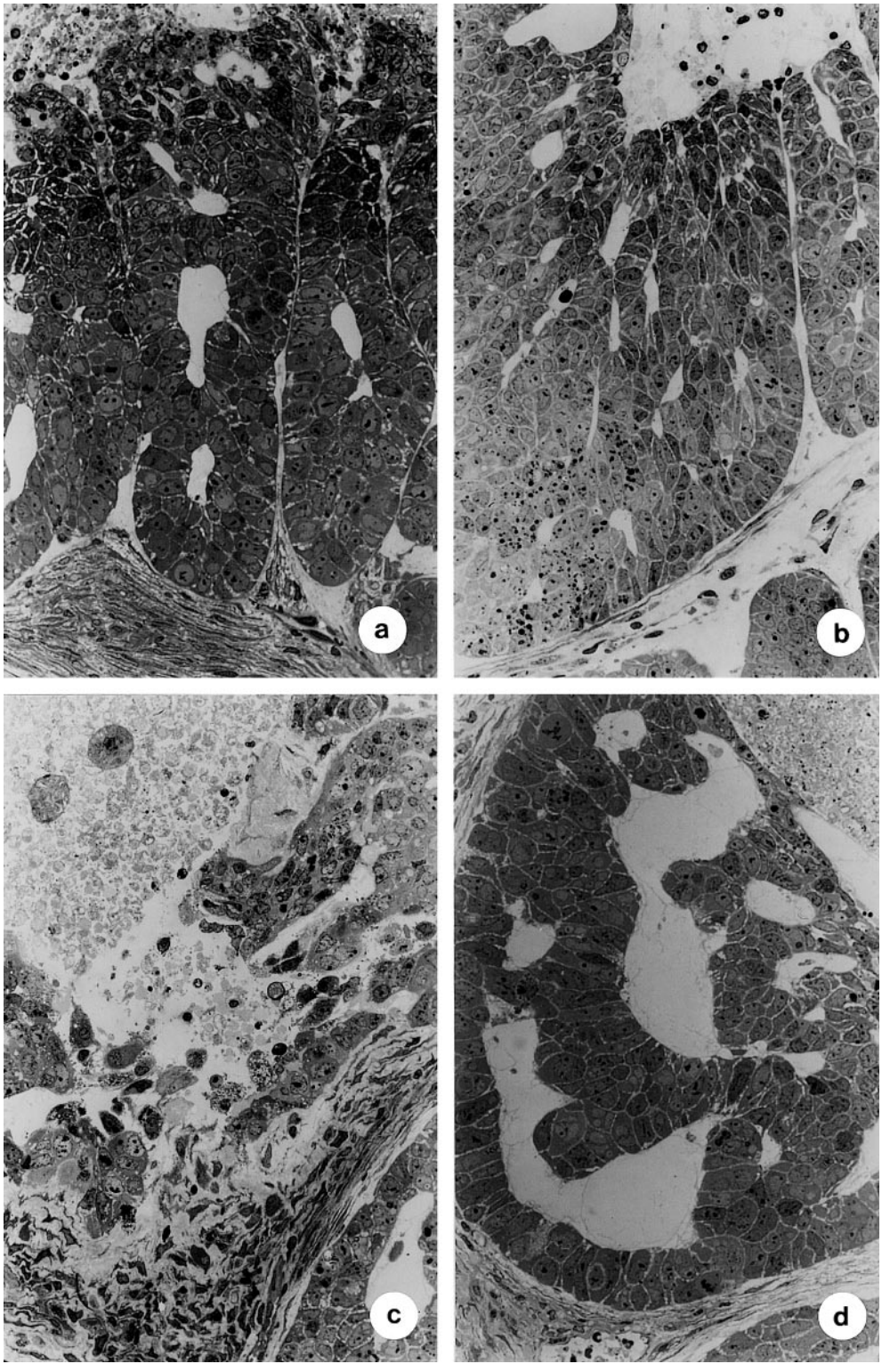

Fig. 4a–d Histological appearance of the untreated human hypopharynx carcinoma xenograft (**a**) and of tumors 24 h (**b**), 72 h (**c**), and 120 h (**d**) after irradiation with 30 Gy. Untreated tumors consist of vital cell cords that are surrounded by connective tissue (**a**, *bottom*) and enclose wide central areas containing necrotic debris (**a**, *top*). Within 24 h after therapy, cytoplasmic inclusion bodies and single-cell necroses appear in many tumor cells (**b**). On day 3, the architecture of the xenograft is almost destroyed, while host-supplied inflammatory cells continue to remove the injured tumor tissue (**c**). Eventually loosened cords of intact carcinoma cells constitute the basis for a regrowth of tumors (**d**). Semithick sections, stained with toluidine blue, ×105

tigators revealed dose-dependent changes (Kristjansen et al. 1990; Murata et al. 1998) or even a drop of the energy status at high irradiation doses (Sijens et al. 1986; Sijens et al. 1997). With regard to the phosphomonoester and phosphodiester regions, conflicting results have been reported. While Majors et al. (1990) and Street and Koutcher (1997) did not detect any change in the PME and PDE levels, others observed decreases of phospholipid metabolites following irradiation (Sakurai et al. 1998; Sijens et al. 1986). The latter phenomenon has also been confirmed in patients (Ng et al. 1989). In contrast, Mahmood et al. (1995) uncovered an increase of the PME and PDE levels in the RIF-1 tumor model after a single dose of 17 Gy.

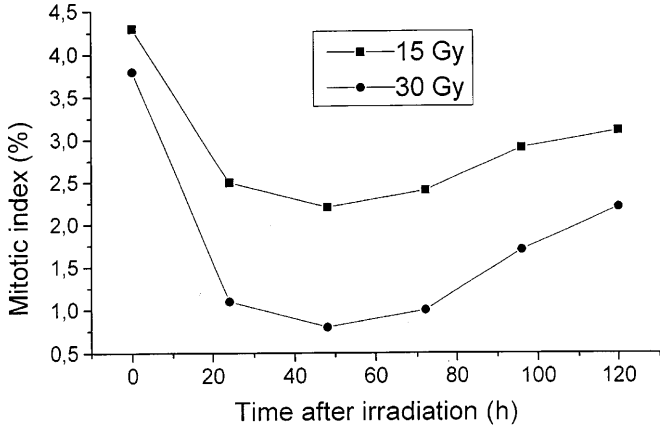

Fig. 5 Mitotic indices found in the hypopharynx carcinoma xenografts following irradiation with 15 Gy and 30 Gy. For each data point, specimens from two animals were evaluated in each case

The results of the present study indicate that the tumor pH, the phosphomonoesters, and the phosphodiesters were the most sensitive post-treatment markers correlating with tumor response to radiotherapy (Fig. 2c). The observed alterations were dose-dependent and only reached significance after irradiation with 30 Gy. The phospholipids PME and PDE are potential precursors of phospholipid synthesis and products of membrane catabolism respectively (Van den Bosch 1974). It has been hypothesized that increased PME levels are associated with intensified cell membrane synthesis and cell proliferation (Maris et al. 1985), while increased PDE levels reflect the formation of necrotic regions in squamous-cell carcinomas (Evanochko et al. 1984). The decline of the PME/TPC ratio as well as the increment of PDE/TPC, both occurring within 2 days after therapy (Fig. 2c), were in line with these hypotheses and, further, corresponded well with the concurrent morphological alterations, i.e. manifestation of necrotic regions and fall in mitotic activity.

The spectral alterations observed in the present study are partly in contrast with the changes previously reported after therapy of the same xenograft with cisplatin (Tausch-Treml et al. 1992a). While the PME/TPC and the PDE/TPC ratios as well as the pH value showed analogous changes in both studies, an increase of the high-energy phosphates phosphocreatine and β-NTP developed under the influence of cisplatin. This phenomenon seemed to be based on an altered tumor blood supply. After chemotherapy, a remarkable dilatation of the capillaries was previously observed within the connective tissue of the hypopharynx carcinoma xenograft (Tausch-Treml et al. 1992a). In the present study, no significant effects of irradiation on the size of the blood vessels or on the energy status of tumors could be detected.

Although the changes of the pH value and the PME/TPC and PDE/TPC ratios were significant following irradiation with 30 Gy, they did not allow prediction of the individual tumor responses to irradiation from the spectral measurements. This becomes obvious in Table 1 (lower part), where the changes of the aforementioned metabolite ratios were correlated with the tumor growth delay observed in the individual tumors after irradiation with 30 Gy. Only the change of the PDE/TPC ratio 24 h and 48 h after treatment showed a fairly good, but insignificant correlation with the tumor response, while there was hardly any relation with the changes of the pH or the PME/TPC ratio. When comparing tumor growth delays with the pre-treatment metabolite ratios, the PME/TPC ratio and the product of PME/TPC and PDE/TPC did significantly correlate with individual tumor responses in the group of mice irradiated with 30 Gy (Table 1, upper part). The pre-treatment PCr/TPC and P_i/TPC ratios as well as the pH values were obviously unrelated to the radiation-induced growth delays. These results are remarkable as they contradict the suggestion that phosphorus compounds involved in energy metabolism reflect the radiobiologically relevant hypoxic fraction of tumor cells and, thus, should be better for predicting radiosensitivity than the phosphomonoesters and phosphodiesters. However, the usefulness of ^{31}P NMR spectroscopy for detecting radiobiologically relevant tumor hypoxia is still unclear. While a number of studies found PCr/TPC and/or NTP/TPC ratios to be positively related to the oxygen level in tumors (Sostman et al. 1991; Vaupel et al. 1989) and – vice versa – negatively related to hypoxic fractions (Fu et al. 1990; Li et al. 1995; Wendland et al. 1992), other authors have been unable to show such a correlation across multiple tumor models (Gerweck et al. 1995; Rofstad et al. 1989). It appears that the levels of energy metabolites vary considerably among different tumor lines, making ^{31}P NMR spectroscopy insufficient to provide an accurate prediction of the hypoxic fraction in individual tumors. Moreover, recent investigations have suggested that tumors can maintain their bioenergetic status even during a period of severe hypoxia if they are able to produce high-energy phosphates by anaerobic glycolysis (Nordsmark et al. 1995, 1997). Thus, the obviously low precision of ^{31}P NMR spectroscopy in measuring tumor hypoxia is the most probable explanation of why the pre-treatment PCr/TPC and NTP/TPC ratios were unrelated to the individual tumor responses in the present study. It is rather unlikely that acute changes in the oxygenation status of tumors occurred between the pre-treatment NMR measurements and irradiation, since both procedures were carried out with a time delay of about 4 h.

In conclusion, it becomes obvious that there is probably no uniform ^{31}P NMR spectroscopic parameter predicting the tumor response to irradiation among different tumor models. In the hypopharynx carcinoma investigated here, high pre-treatment PME/TPC and PDE/TPC ratios correlated with short growth delays of individual tumors much better than any other parameter. Since they significantly increased with tumor size, it is suggested that elevated levels of both parameters might indicate a development of necrotic regions and,

thus, an enlargement of the hypoxic cell fraction within the tumor tissue. However, a correlation between pretreatment levels of high-energy phosphates and tumor responses could not be established, although the PCr/TPC ratio was found to decrease significantly with tumor size. In view of these disappointing results, a search for other parameters that may predict radiosensitivity of tumors better than cellular phosphate compounds seems to be required. Promising approaches include the analysis of genes involved in the regulation of apoptosis (Jäckel 1998) and determination of polyamine levels in tumor tissues, which are known to protect cells from free-radical damage (Ha et al. 1998).

References

Evanochko WT, Ng CT, Glickson JD (1984) Applications of in vivo NMR spectroscopy to cancer. Magn Reson Med 1: 508–534

Fu KK, Wendland MF, Iyer SB, Lam KN, Engeseth H, James TL (1990) Correlations between in vivo ^{31}P NMR spectroscopy measurements, tumor size, hypoxic fraction and cell survival after radiotherapy. Int J Radiat Oncol Biol Phys 18: 1341–1350

Gerweck LE, Koutcher J, Zaidi ST (1995) Energy status parameters, hypoxia fraction and radiocurability across tumor types. Acta Oncol 34: 335–338

Ha HC, Sirisoma NS, Kuppusamy P, Zweier JL, Woster PM, Casero RA (1998) The natural polyamine spermine functions directly as a free radical scavenger. Proc Natl Acad Sci USA 95: 11140–11145

Jäckel MC (1998) Genetic control of programmed cell death (apoptosis). HNO 46: 614–625

Karczmar GS, Meyerhoff DJ, Boska MD, Hubesch B, Poole J, Matson GB, Valone F, Weiner MW (1991) ^{31}P spectroscopy study of response of superficial human tumors to therapy. Radiology 179: 149–153

Kristjansen PEG, Pedersen EJ, Quistorff B, Elling F, Spang-Thomsen M (1990) Early effects of radiotherapy in small cell lung cancer xenografts monitored by ^{31}P magnetic resonance spectroscopy and biochemical analysis. Cancer Res 50: 4880–4884

Li SJ, Jin GY, Fish BL, Moulder JE (1995) Correlation of radiobiological assays of hypoxic fraction with phosphorus-31 magnetic resonance spectroscopy across multiple tumor lines. Radiat Res 143: 45–53

Mahmood U, Alfieri AA, Ballon D, Traganos F, Koutcher JA (1995) In vitro and in vivo ^{31}P nuclear magnetic resonance measurements of metabolic changes post radiation. Cancer Res 55: 1248–1254

Majors AW, Ng TC, Karalis IM, Edinger MG, Tubbs RR, Higgins PD, Shin KH (1990) Phosphorus metabolites and the distribution of cell cycle phase of RIF-1 tumors in response to 14 Gy irradiation. Magn Reson Med 16: 425–430

Maldonado X, Alonso J, Giralt J, Cucurella MG, del Campo JM, Rovira A, Felip E, Capellades J, Grive E, Rubio D, Gili J (1998) 31 Phosphorus magnetic resonance spectroscopy in the assessment of head and neck tumors. Int J Radiat Oncol Biol Phys 40: 309–312

Maris JM, Evans AE, McLaughlin AC, Dangio GJ, Bolinger L, Manos H, Chance B (1985) ^{31}P NMR spectroscopic investigation of human neuroblastoma in situ. N Engl J Med 312: 1500–1505

Merchant TE, Alfieri AA, Glonek T, Koutcher JA (1995) Comparison of relative changes in phosphatic metabolites and phospholipids after irradiation. Radiat Res 142: 29–38

Murata O, Sakurai H, Mitsuhashi N, Hasegawa M, Yamakawa M, Kurosaki H, Hayakawa K, Niibe H (1998) ^{31}P NMR spectroscopy can predict the optimum interval between fractionated irradiation doses. Anticancer Res 18: 4297–4302

Ng TC, Grundfest S, Vijayakumar S, Baldwin NJ, Majors AW, Karalis I, Meaney TF, Shin KH, Thomas FJ, Tubbs R (1989) Therapeutic response of breast carcinoma monitored by ^{31}P MRS in situ. Magn Reson Med 10: 125–134

Nordsmark M, Grau C, Horsman MR, Stödkilde Jörgensen H, Overgaard J (1995) Relationship between tumor oxygenation, bioenergetic status and radiobiological hypoxia in an experimental model. Acta Oncol 34: 329–334

Nordsmark M, Maxwell RJ, Horsman MR, Bentzen SM, Overgaard J (1997) The effect of hypoxia and hyperoxia on nucleoside triphosphate/inorganic phosphate, pO_2, and radiation response in an experimental tumour model. Br J Cancer 76: 1432–1439

Rofstad EK, DeMuth P, Fenton BM, Ceckler TL, Sutherland RM (1989) ^{31}P NMR spectroscopy and HbO_2 cryospectrophotometry in prediction of tumor radioresistance caused by hypoxia. Int J Radiat Oncol Biol Phys 16: 919–923

Sakurai H, Mitsuhashi N, Murata O, Kitamoto Y, Saito Y, Hasegawa M, Akimoto T, Takahashi T, Nasu S, Niibe H (1998) Early radiation effects in highly apoptotic murine lymphome xenografts monitored by ^{31}P magnetic resonance spectroscopy. Int J Radiat Oncol Biol Phys 41: 1157–1162

Sijens PE, Bovee WMM, Seijkens D, Los G, Rutgers DH (1986) In vivo ^{31}P NMR study of the response of a murine mammary tumor to different doses of gamma-radiation. Cancer Res 46: 1427–1432

Sijens PE, Baldwin NJ, Ng TC (1997) ^{31}P magnetic resonance spectroscopy detection of response-predictive adenosine triphosphate decrease in irradiated radiation-induced fibrosarcoma-1 tumors. Invest Radiol 32: 39–43

Snow GB (1992) Evaluation and staging. In: Snow GB, Clark JR (eds) Multimodality therapy for head and neck cancer, 1st edn. Thieme, Stuttgart New York, pp 3–44

Sostman HD, Rockwell SR, Sylvia AL, Madwed D, Cofer G, Charles HC, Negro-Vilar R, Moore D (1991) Evaluation of BA1112 rhabdomyosarcoma oxygenation with microelectrodes, optical spectrophotometry, radiosensitivity and magnetic resonance spectroscopy. Magn Reson Med 20: 253–267

Street JC, Koutcher JA (1997) Effect of radiotherapy and chemotherapy on composition of tumor membrane phospholipids. Lipids 32: 45–49

Tausch-Treml R, Köpf-Maier P, Baumgart F, Gewiese B, Ziessow D, Scherer H, Wolf KJ (1991) ^{31}P NMR spectroscopy, histology and cytokinetics of a xenografted hypopharynx carcinoma following treatment with cisplatin: comparison of three sublines with increasing resistance. Br J Cancer 64: 485–493

Tausch-Treml R, Baumgart F, Ziessow D, Köpf-Maier P (1992a) ^{31}P NMR spectroscopy of a xenografted hypopharynx carcinoma: effects of tumor growth and treatment with cisplatin on the tumor phosphorus metabolism, histology and cytokinetics. NMR Biomed 5: 127–136

Tausch-Treml R, Baumgart F, Jäckel M, Gewiese B, Scherer H, Wolf KJ (1992b) ^{31}P NMR spectroscopy study of response of head and neck carcinomas to therapy. In: Abstracts of the SMRM 10th Annual Meeting, Berlin, p 3612

Van den Bosch H (1974) Phosphoglyceride metabolism. Annu Rev Biochem 43: 243

Vaupel P, Okunieff P, Kallinowski F, Neuringer LJ (1989) Correlations between ^{31}P NMR spectroscopy and tissue O_2 tension measurements in a murine fibrosarcoma. Radiat Res 120: 477–493

Vogl T, Peer F, Schedel H, Reiman V, Holtmann S, Rennschmid C, Sauter R, Lissner J (1989) ^{31}P spectroscopy of head and neck tumors – surface coil technique. Magn Reson Imag 7: 425–435

Wendland MF, Iyer SB, Fu KK, Lam KN, James TL (1992) Correlations between in vivo ^{31}P MRS measurements, tumor size, cell survival, and hypoxic fraction in the murine EMT6 tumor. Magn Reson Med 25: 217–232